

CaBP1, a neuronal Ca²⁺ sensor protein, inhibits inositol trisphosphate receptors by clamping intersubunit interactions

Congmin Li^{a,1}, Masahiro Enomoto^{b,1}, Ana M. Rossi^{c,1}, Min-Duk Seo^{b,1,2}, Taufiq Rahman^c, Peter B. Stathopoulos^b, Colin W. Taylor^{c,3}, Mitsuhiro Ikura^{b,3}, and James B. Ames^{a,3}

^aDepartment of Chemistry, University of California, Davis, CA 95616; ^bDivision of Signaling Biology, Ontario Cancer Institute and Department of Medical Biophysics, University of Toronto, Toronto, ON, Canada M5G 1L7; and ^cDepartment of Pharmacology, University of Cambridge, Cambridge CB2 1PD, United Kingdom

Edited by Chikashi Toyoshima, University of Tokyo, Tokyo, Japan, and approved April 9, 2013 (received for review December 3, 2012)

Calcium-binding protein 1 (CaBP1) is a neuron-specific member of the calmodulin superfamily that regulates several Ca²⁺ channels, including inositol 1,4,5-trisphosphate receptors (InsP₃Rs). CaBP1 alone does not affect InsP₃R activity, but it inhibits InsP₃-evoked Ca²⁺ release by slowing the rate of InsP₃R opening. The inhibition is enhanced by Ca²⁺ binding to both the InsP₃R and CaBP1. CaBP1 binds via its C lobe to the cytosolic N-terminal region (NT; residues 1–604) of InsP₃R1. NMR paramagnetic relaxation enhancement analysis demonstrates that a cluster of hydrophobic residues (V101, L104, and V162) within the C lobe of CaBP1 that are exposed after Ca²⁺ binding interact with a complementary cluster of hydrophobic residues (L302, I364, and L393) in the β -domain of the InsP₃-binding core. These residues are essential for CaBP1 binding to the NT and for inhibition of InsP₃R activity by CaBP1. Docking analyses and paramagnetic relaxation enhancement structural restraints suggest that CaBP1 forms an extended tetrameric turret attached by the tetrameric NT to the cytosolic vestibule of the InsP₃R pore. InsP₃ activates InsP₃Rs by initiating conformational changes that lead to disruption of an intersubunit interaction between a “hot-spot” loop in the suppressor domain (residues 1–223) and the InsP₃-binding core β -domain. Targeted cross-linking of residues that contribute to this interface show that InsP₃ attenuates cross-linking, whereas CaBP1 promotes it. We conclude that CaBP1 inhibits InsP₃R activity by restricting the intersubunit movements that initiate gating.

EF hand | intracellular Ca²⁺ channel | ion channel | ryanodine receptor

Dynamic increases in cytosolic free Ca²⁺ concentration ([Ca²⁺]_c) regulate many cellular events, including acute and long-term changes in neuronal activity (1–3). Release of Ca²⁺ from intracellular stores is controlled by intracellular Ca²⁺ channels (4), the most common of which are inositol 1,4,5-trisphosphate receptors (InsP₃Rs) (5, 6). Dual regulation of InsP₃Rs by InsP₃ and Ca²⁺ facilitates regenerative Ca²⁺ release (6), generating Ca²⁺ signals of remarkable versatility and spatiotemporal complexity (1, 2, 7). The sites through which Ca²⁺ biphasically regulates InsP₃Rs are unresolved (5, 8, 9). There is, however, evidence, that proteins with EF-hand Ca²⁺-binding motifs can regulate gating of InsP₃Rs. These include calmodulin (CaM) (10–12), calmyrin (CIB1) (13), and neuronal Ca²⁺ sensor (NCS) proteins (2). The latter comprise a branch of the CaM superfamily that includes NCS-1 (14) and Ca²⁺-binding protein 1 (CaBP1) (15, 16).

CaBP1–5 proteins (2, 17) have four EF hands that form pairs within the N lobe (EF1 and 2) and C lobe (EF3 and 4). The two lobes are structurally independent (18) and connected by a flexible linker (18). Whereas all four EF hands bind Ca²⁺ in CaM, EF2 in CaBP1 does not bind Ca²⁺, and EF1 has reduced selectivity for Ca²⁺ over Mg²⁺. EF3 and EF4 in the C lobe of CaBP1 exhibit canonical Ca²⁺-induced conformational changes (18, 19). Many splice variants and isoforms of CaBPs are expressed in different neurons (20–22), and their targets include a variety of ion channels (2). CaBP1, for example, regulates voltage-gated P/Q-type

(23) and L-type Ca²⁺ channels (24) and a transient receptor potential channel, TRPC5 (25). Furthermore, the prevailing view that InsP₃Rs open only after binding InsP₃ was challenged by evidence that CaBP1 (15) and related proteins (13) might, in their Ca²⁺-bound forms, gate InsP₃Rs. The suggestion that Ca²⁺, via CaBP1, might directly gate InsP₃Rs proved to be contentious, but it spawned further evidence that CaBP1 regulates InsP₃Rs (14, 16, 20).

InsP₃Rs are large tetrameric channels (5, 6). Their activation is initiated within the N-terminal domain (NT; residues 1–604) by binding of InsP₃ to the InsP₃-binding core (IBC; residues 224–604) of each subunit (26). This process leads, via rearrangement of the suppressor domain (SD; residues 1–223) (27), to opening of an intrinsic pore (28, 29). Despite extensive studies of CaBP1 (2) and of the many proteins that modulate InsP₃Rs (5), little is known about the structural basis of these protein interactions with InsP₃Rs or of CaBP1 with any ion channel. Here we combine NMR, mutagenesis, cross-linking, and functional analyses to define, at the atomic level, the interactions between CaBP1 and InsP₃Rs.

Results

CaBP1 Inhibits InsP₃-Evoked Ca²⁺ Release. CaBP1 is found only in neurons (2), and they predominantly express InsP₃R1. We therefore used permeabilized DT40 cells lacking endogenous InsP₃Rs, but stably expressing rat InsP₃R1, to assess the effects of CaBP1 on Ca²⁺ release from intracellular stores. The two splice variants of CaBP1 expressed in brain (17) regulate InsP₃Rs and Ca²⁺ channels similarly (16). Throughout this study, we used the short variant (Table S1) because its solubility makes it more amenable to NMR analysis. Across a range of [Ca²⁺]_c, CaBP1 alone had no effect on the Ca²⁺ content of the intracellular stores of DT40–InsP₃R1 cells (Fig. S1 A–D). The lack of effect of Ca²⁺–CaBP1 on InsP₃R1 was confirmed by nuclear patch-clamp analyses of single InsP₃R1 (Fig. S1E). These results are inconsistent with the notion that Ca²⁺–CaBP1 stimulates Ca²⁺ release via InsP₃R (15), a suggestion that has also been challenged by others, who argue that CaBP1 inhibits InsP₃-evoked Ca²⁺ release (16, 20).

CaBP1 caused a concentration-dependent decrease in the sensitivity of InsP₃-evoked Ca²⁺ release (Fig. 1A and Table S2) without affecting ³H–InsP₃ binding (Fig. S1 G–I). Inhibition of

Author contributions: C.W.T., M.I., and J.B.A. designed research; C.L., M.E., A.M.R., M.-D.S., T.R., and P.B.S. performed research; C.L., M.E., A.M.R., M.-D.S., T.R., P.B.S., C.W.T., M.I., and J.B.A. analyzed data; and C.L., C.W.T., M.I., and J.B.A. wrote the paper.

The authors declare no conflict of interest.

This article is a PNAS Direct Submission.

Freely available online through the PNAS open access option.

¹C.L., M.E., A.M.R., and M.-D.S. contributed equally to this work.

²Present address: Department of Pharmacy, Ajou University, Suwon 443-749, Korea.

³To whom correspondence may be addressed. E-mail: jbam@ucdavis.edu, mikura@uhnres.utoronto.ca, or cwt1000@cam.ac.uk.

This article contains supporting information online at www.pnas.org/lookup/suppl/doi:10.1073/pnas.1220847110/-DCSupplemental.

InsP₃-evoked Ca²⁺ release by CaBP1 was increased at higher [Ca²⁺]_c, but was evident even at the [Ca²⁺]_c of a resting cell, although not at lower [Ca²⁺]_c (Fig. 1*B* and Table S2). In single-channel analyses recorded under optimal conditions for InsP₃R activation (30), CaBP1 (10 μM) massively reduced channel activity (*NP*_o) without affecting unitary conductance (*γ*_{Cs}) or mean channel open time (*τ*_o) (Fig. 1*C* and *D*). Analysis of records that included only a single functional InsP₃R established that an increase in mean channel closed time (*τ*_c) from 4.2 ± 0.9 ms to 46 ± 13 ms accounted for the 5.3-fold reduction in *NP*_o in the presence of CaBP1 (Fig. S1*F*). The lack of effect on *τ*_o and *γ*_{Cs} indicates that CaBP1 inhibits gating rather than blocking the InsP₃R pore.

Inhibition of InsP₃R by CaBP1 Is Enhanced by Ca²⁺ Binding to both CaBP1 and InsP₃R. Cytosolic Ca²⁺ enhances the inhibition of InsP₃R by CaBP1 (Fig. 1*B* and Table S2). We mutated residues within each of the three functional EF hands of CaBP1 to prevent Ca²⁺ binding (CaBP1₁₃₄) (Fig. S2*F*). CaBP1₁₃₄ was as effective as CaBP1 in causing Ca²⁺-dependent inhibition of InsP₃-evoked Ca²⁺ release at the typical [Ca²⁺]_c of a resting cell (230 nM), but less effective than CaBP1 at higher [Ca²⁺]_c (Fig. 1*B* and Fig. S2*A–D*). When only the last pair of EF hands was mutated (CaBP1₃₄), the results were similar to those obtained with CaBP1₁₃₄ (Fig. S2*E*). Although CaBP1₁₃₄ does not bind Ca²⁺ (Fig. S2*F*), its ability to inhibit InsP₃-evoked Ca²⁺ release was enhanced by increasing [Ca²⁺]_c. However, at the highest [Ca²⁺]_c, the inhibition by mutant CaBP1 was less than with native CaBP1 (Fig. 1*B* and Fig. S2). This result suggests that the last pair of EF hands in CaBP1 contributes to the enhanced inhibition of InsP₃R at elevated [Ca²⁺]_c. We conclude that CaBP1 inhibits InsP₃-evoked Ca²⁺ release at resting [Ca²⁺]_c. At the [Ca²⁺]_c of stimulated cells, the inhibition is potentiated by Ca²⁺ binding to both InsP₃R and the last pair of EF hands in CaBP1. This complex regulation of CaBP1–InsP₃R interactions by cytosolic Ca²⁺ may have contributed to conflicting reports of their Ca²⁺ dependence (13, 15, 16, 20) and requirement for functional EF hands (15, 16).

Local Hydrophobic Interactions Between InsP₃R and the C Lobe of CaBP1. Ca²⁺–CaBP1 binds via its C lobe to the NT, in both its apo and InsP₃-bound forms, with a 1:1 stoichiometry and an equilibrium dissociation constant (*K*_D) of ~3 μM (18). In the absence of Ca²⁺, CaBP1 binds with 10-fold lower affinity (18), consistent with our functional analyses (Fig. 1*B*). We used NMR-based approaches, including chemical shift perturbation and paramagnetic relaxation enhancement (PRE) (31), to examine

the structure of the NT–CaBP1 complex. Our PRE experiments measure distances between side-chain methyl groups in CaBP1 that are <10 Å away from nitroxide spin labels attached to specific Cys residues in the NT. The starting point was the NT in which all Cys residues were replaced by Ala (NT^{CL}) (Table S1). Extensive structural and functional studies confirmed that NT^{CL} mimics the behavior of wild-type NT (29). Isothermal titration calorimetry demonstrated that Ca²⁺–CaBP1 binds to NT^{CL} (*K*_D = 16 μM, *pK*_D = 4.8 ± 0.1) (Fig. S3*A*), although with lower affinity than native NT (*K*_D = 3 μM, *pK*_D = 5.5 ± 0.1) (18). This small difference in Gibbs free energy of binding ($\Delta\Delta G^\circ = 0.9$ kcal/mole) suggests that CaBP1 has a similar structural interaction with NT and NT^{CL}, consistent with the similar NMR spectra of Ca²⁺–CaBP1 bound to NT^{CL} (Fig. S4*A*, red) and wild-type NT (Fig. S4*A*, blue). We then introduced single Cys residues into strategic sites on the surface of NT^{CL} and used them in PRE experiments. The NMR spectra of CaBP1 bound to wild-type and mutant NTs are similar, confirming that each NT mutant is folded and bound similarly to CaBP1.

Binding of NT^{CL} to ¹⁵N-labeled CaBP1 caused nearly all backbone amide resonances to broaden beyond detection in ¹⁵N–¹H heteronuclear single quantum coherence spectra, preventing use of backbone amide resonances in the PRE analysis. Only side-chain methyl NMR resonances of CaBP1 were detected with enough sensitivity to be analyzed using PRE. ¹³C-labeled CaBP1 binding to unlabeled NT^{CL} was monitored by using ¹H–¹³C methyl transverse relaxation-optimized spectroscopy (TROSY) NMR (Fig. S4*A*). Binding of NT^{CL} had large effects on the NMR resonances assigned to CaBP1 residues in the C lobe, whereas residues in the N lobe were unaffected. This finding is consistent with the NT binding via the C lobe of CaBP1 (18). The ¹³C-labeled methyl resonances of V101, L104, and V162 in CaBP1 became severely broadened after the addition of NT^{CL}, suggesting that these residues directly contact NT^{CL}. Mutation of each of these residues to Ser massively reduced the affinity of CaBP1 for NT^{CL} (Fig. S3*B* and *C*). In addition, exposed residues in CaBP1 (I124, L131, L132, and L150) have methyl resonances that show perturbations in chemical shifts, indicating a change in their magnetic environment upon binding of the NT. By monitoring the NMR spectral changes of ¹³C-methyl-labeled CaBP1 complexed with NT^{CL} in the presence (paramagnetic) and absence (diamagnetic) of attached spin label, the proximity of NT^{CL} and CaBP1 was defined. A methyl TROSY spectrum of ¹³C-labeled CaBP1 bound to NT^{CL} with a single Cys insertion, NT^{CL}(E20C), was similar to that of CaBP1 bound to NT^{CL} (Fig. S4*A* and *B*), indicating that NT^{CL}(E20C) is structurally intact. Attachment of a nitroxide

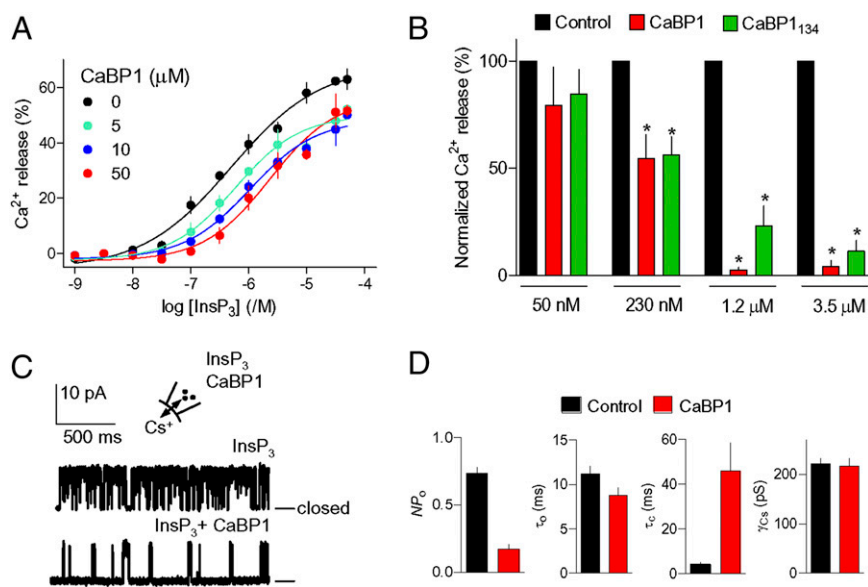


Fig. 1. Inhibition of InsP₃R by CaBP1. (A) CaBP1 inhibits InsP₃-evoked Ca²⁺ release. Permeabilized DT40–IP₃R1 cells in CLM with a [Ca²⁺]_c of 1.2 μM were incubated with CaBP1 (10 min) before adding InsP₃. Results (means ± SEM; *n* = 3, with duplicate determinations in each) show the concentration-dependent release of Ca²⁺ by InsP₃. (B) Effects of CaBP1 and CaBP1₁₃₄ (50 μM) on InsP₃-evoked Ca²⁺ release at the indicated [Ca²⁺]_c show that CaBP1 is not the only Ca²⁺ sensor. For each [Ca²⁺]_c, results (percentage of control, means ± SEM; *n* = 3–4, with duplicate determinations in each) show the Ca²⁺ release evoked by the concentration of InsP₃ that evoked half-maximal Ca²⁺ release (*EC*₅₀) under control conditions. **P* < 0.05 relative to control. (C) Typical patch-clamp recordings from single InsP₃R1 in medium with [Ca²⁺]_c of 1.5 μM stimulated with InsP₃ (10 μM) alone or with CaBP1 (10 μM). Bars show the closed state. The holding potential was +40 mV. (D) Summary data (mean ± SEM; *n* given in Fig. S1*F*) show *NP*_o, mean channel open (*τ*_o) and closed (*τ*_c) times and unitary conductance (*γ*_{Cs}).

spin label to NT^{CL}(E20C) caused a marked decrease in NMR peak intensity for some CaBP1 residues (I124, L131, L132, V148, and L150), whereas others (L99, V136, L141, L145, and V156) were less affected (Fig. S4B). The ratios of peak intensities in the presence and absence of spin label ($I_{\text{Paramagnetic}}/I_{\text{Diamagnetic}}$) were taken as a measure of the distance between the methyl groups and spin label. The PRE ratios are listed for all single Cys insertions in Fig. S4C.

We used the PRE restraints and chemical shift perturbation data within HADDOCK (32) to dock the NMR structure of Ca²⁺-bound C lobe of CaBP1 (18) onto the crystal structure of the NT (29) (Fig. 2A). Within the complex, the Ca²⁺-bound C lobe of CaBP1 is in the familiar open conformation typical of Ca²⁺-bound EF hands in CaM (33). Exposed hydrophobic residues in Ca²⁺-CaBP1 (V101, L104, and V162) interact with clustered hydrophobic residues (L302, I364, and L393) in the IBC- β domain of InsP₃R1 (Fig. 2A). These residues are conserved in InsP₃Rs but not in ryanodine receptors, consistent with evidence that CaBP1 binds to all three InsP₃R subtypes (15, 16) but not to ryanodine receptors (16). Exposed CaBP1 residues in EF4 (I144, M164, and M165) made contacts with H289 in the IBC- β domain, and side-chain atoms of R167 (CaBP1) were within 5 Å of conserved residues (N47 and N48) in the SD. These interactions align with evidence that CaBP1 binding to InsP₃R is mediated by the NT (15) and with both the IBC and SD being required for high-affinity binding (16, 18). The key hydrophobic residues in CaBP1 (V101, L104, and V162) are less exposed in the closed conformation of Ca²⁺-free CaBP1, consistent with the reduced affinity of CaBP1 for NT in the absence of Ca²⁺ (18). The importance of the hydrophobic residues within the IBC was confirmed by mutagenesis. A triple mutant of NT^{CL} (L302S/I364S/L393S) bound InsP₃, but not CaBP1 (Fig. S5A–C), confirming that InsP₃ and CaBP1 bind to distinct sites (18). Interaction of the NT with Ca²⁺-CaBP1 via localized clusters of hydrophobic residues probably explains why mutation of single residues in CaBP1 (V101S, L104S, and V162S) massively attenuates its binding to the NT (Fig. S3B and C).

CaBP1 Forms a Ring Around the Cytosolic Entrance of the InsP₃R. Native InsP₃R is a tetramer with a central ion-conducting pore (34). Docking crystal structures of the NT (29) onto a cryo-EM structure of full-length tetrameric InsP₃R1 (34) suggests the arrangement shown in Fig. 2B, which is similar to that proposed for ryanodine receptors (35). Overlaying the structure of the CaBP1/NT complex onto the tetrameric NT generates a structure in which four molecules of CaBP1 associate, via the clustered hydrophobic residues in their C lobes, with the three clustered hydrophobic residues in each of the four IBC- β domains. The latter contribute to the lining of the central cytosolic vestibule, and the four molecules of CaBP1 form a ring-like structure around it. The position of the N lobe of CaBP1 within the tetrameric complex could not be defined because NMR signals assigned to it were unaffected by the NT. Previous studies showed that CaBP1 and its isolated C lobe bind to the NT with very similar affinity (18), consistent with an absence of contacts between the NT and N lobe. The location of the N lobe within the complex was estimated by first generating an ensemble of full-length CaBP1 structures in which the two lobes are connected by a flexible linker and are free to adopt many different relative orientations during simulated annealing. This ensemble of full-length CaBP1 structures was then docked into the NT structure (Fig. S4E). The CaBP1 C-lobe interaction with the NT is well defined in the ensemble of docked structures (cyan in Fig. S4E with rmsd = 0.5 Å), whereas the relative location of the N lobe in the complex is highly variable (Fig. S4E, blue). Each structure from the ensemble was then overlaid and docked into the tetrameric NT structure. The lowest energy model (Fig. 2C) placed the N lobe above the C lobe and projecting into the cytosol away from any contact with the NT. This elongated organization of the two lobes of CaBP1 differs from their compact, hexameric arrangement in the CaBP1 crystal structure (19).

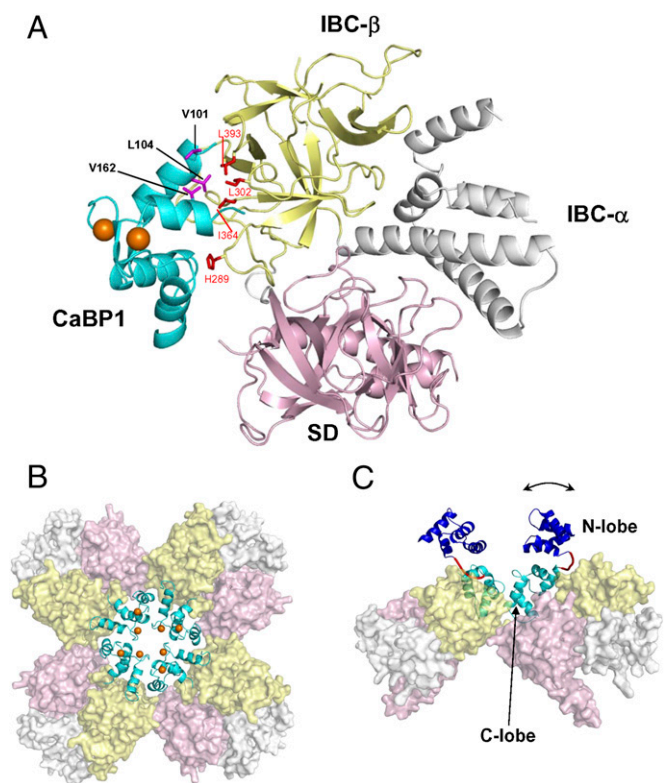


Fig. 2. Structure of CaBP1 bound to InsP₃R. (A) The C lobe of Ca²⁺-bound CaBP1 [cyan; Protein Data Bank (PDB) ID code 2K7D] bound to NT (PDB ID code 3UJ4) in a 1:1 complex. Key residues at the binding interface are highlighted in magenta (CaBP1) and red (InsP₃R). NT subdomains are colored pink (SD), yellow (IBC- β), and gray (IBC- α). (B) Model of tetrameric NT (pink, yellow, and gray) generated by superimposing the NT crystal structure (29) onto a cryo-EM structure of InsP₃R1 (34). NMR structural restraints were used to define contacts between each NT and C lobe of CaBP1 (cyan, with Ca²⁺ in orange). (C) Side view of tetrameric NT bound to full-length CaBP1 in a 4:4 complex. The N lobe of CaBP1 (blue) is connected to the C lobe (cyan) by a flexible linker (red) that allows the N lobe to adopt multiple orientations (indicated by the arrow).

Solution NMR has shown that, as with CaM (36) and troponin C (37), the CaBP1 N and C lobes fold independently and do not interact structurally (18). This finding is consistent with a lack of contact between the lobes of CaBP1 when complexed with InsP₃R (Fig. 2C).

Functional analyses confirmed the importance of the critical residues within CaBP1. CaBP1 with mutations to the key hydrophobic residues [CaBP1(V101S/L104S) or CaBP1(V162S)] (Fig. 2A) had no effect on InsP₃-evoked Ca²⁺ release at any [Ca²⁺]_c examined, even when the CaBP1 concentrations were increased to 100 μ M (Fig. 3A, Fig. S5D, and Table S3). Furthermore, the mutant CaBP1s did not affect inhibition of InsP₃-evoked Ca²⁺ release by CaBP1 (Fig. 3B and Fig. S5E), confirming that they do not compete with CaBP1 for binding to InsP₃Rs. Furthermore, in patch-clamp analyses of nuclear InsP₃R, responses to InsP₃ were unaffected by CaBP1(V162S) (Fig. 3C and Fig. S1F). These functional analyses support the proposed structure of CaBP1 bound to InsP₃R (Fig. 2).

CaBP1 Stabilizes Interactions Between the NTs of Tetrameric InsP₃R. Activation of InsP₃R is proposed to begin with InsP₃-stimulated rearrangement of an intersubunit interface between the SD and IBC- β domain. This movement then disrupts interaction of the “hot-spot” (HS) loop (residues 165–180) of the SD with the IBC- β domain of an adjacent subunit leading to channel gating (29) (Fig. 4A). This model predicts key interactions at the intersubunit interfaces, notably between residues within the SD (K168, L169,

and R170) and IBC (T373, T374, D426, K427). We tested this prediction by inserting pairs of Cys residues into NT^{CL} and assessing their proximity by oxidative cross-linking with copper-phenanthroline (CuP). Three double Cys-substituted mutants (L169C/T373C, L169C/T374C, and K168C/K427C) were engineered as candidates for cross-linking in light of the modeled intersubunit interface (Fig. 4A). NT^{CL}(L169C/T373C) provided the most convincing evidence of a concentration- and time-dependent formation of tetramers in the presence of CuP (Fig. S6A and B). NT^{CL} or NT^{CL} with a single Cys insertion (L169C or T373C) or a pair of Cys that are not expected to be in proximity (A61C/A553C) did not produce tetramers (Fig. S6C). These results confirm the proximity of L169C/T373C to the tetrameric NT interface and demonstrate the utility of CuP cross-linking for analyses of intersubunit interactions between NTs. We used NT^{CL}(L169C/T373C) for subsequent analyses and confirmed that its InsP₃-binding affinity was similar to that of NT^{CL} (Fig. S6D).

InsP₃R activation proceeds via disruption of intersubunit interactions between NT domains (29). Our structure shows CaBP1 forming a tetrameric cap tethered to the NTs of the tetrameric InsP₃R (Fig. 2B). This structure suggests that CaBP1 may lock InsP₃Rs in a closed state by restricting the usual InsP₃-evoked disruption of intersubunit interactions. We used CuP cross-linking and NT^{CL} (L169C/T373C) to assess this possibility. As predicted by our model, InsP₃ caused a concentration-dependent inhibition of CuP-mediated formation of cross-linked tetrameric NT^{CL}(L169C/T373C) (Fig. 4B, Fig. S6E, and Table S4). The biologically inactive isomer of InsP₃ (L-InsP₃) had no

effect on cross-linking (Fig. 4B). In contrast, the C lobe of CaBP1, which lacks endogenous Cys, caused a concentration-dependent increase in the rate and extent of formation of cross-linked tetrameric NT^{CL}(L169C/T373C) (Fig. 4C, Fig. S6F, and Table S4). Similar results were obtained with a Cys-less form of full-length CaBP1 (CaBP1^{CL}) (Fig. 4C, Fig. S6F, and Table S4). These results demonstrate that the C lobe of CaBP1 is largely responsible for the observed effects on NT cross-linking. The CaBP1 C lobe in the absence of Ca²⁺ had no effect on NT tetramer cross-linking (Fig. 4D, Fig. S6G, and Table S4), and neither did CaBP1(V162S), which did not bind the NT (Fig. S6H and Table S4). CaBP1 also partially blocked the inhibition of cross-linking by InsP₃ (Fig. 4E, Fig. S6I, and Table S4). These results (Fig. 4F and Table S4) support our suggestion that InsP₃ activates InsP₃R by disrupting an intersubunit interface between the SD and IBC-β. We suggest that, in the presence of Ca²⁺, CaBP1 forms a tetrameric cap on the InsP₃R that restricts these intersubunit movements and thereby stabilizes a closed state of the channel (Fig. 4G).

Discussion

Gating of InsP₃Rs is regulated by InsP₃ binding, but modulated by many additional signals, notably Ca²⁺ and a variety of proteins (5), including such Ca²⁺-regulated proteins as CaM (12), CIB1 (13), and CaBP1 (2). These proteins are either highly (CaM) or exclusively (CaBP1) expressed in neurons, where they have been proposed to attenuate basal InsP₃R activity (12), provide the Ca²⁺ sensor for inhibitory feedback of InsP₃Rs (5, 11), modulate InsP₃R activity (5), or, for CaBP1 and CIB1, allow Ca²⁺ directly to gate InsP₃Rs (5, 13). The latter suggested that, within neurons, InsP₃Rs, like ryanodine receptors, might mediate regenerative Ca²⁺ signals without the need for coincident production of InsP₃. Our results demonstrate that CaBP1 does not directly activate InsP₃R1, the predominant InsP₃R subtype in neurons (Fig. S1A–D). CaBP1 does, however, massively reduce InsP₃-activated InsP₃R activity by stabilizing a closed state of the channel (Fig. 1C and D), an effect that is enhanced by Ca²⁺ binding to both CaBP1 and the InsP₃R (or a protein tightly associated with InsP₃R). These dual effects of Ca²⁺ may allow cooperative inhibition of InsP₃Rs by increases in [Ca²⁺]_c. However, even at resting [Ca²⁺]_c, there is detectable inhibition of InsP₃Rs by CaBP1 (Fig. 1B and Table S3), suggesting that CaBP1 may also contribute to setting the basal sensitivity of neuronal InsP₃Rs.

We identified hydrophobic residues within the C lobe of CaBP1 that become more exposed when CaBP1 binds Ca²⁺ (V101, L104, and V162) and showed by both NMR and functional analyses that they make essential contacts with hydrophobic residues in the IBC-β domain (L302, I364, and L393) (Fig. 2A). Additional minor contacts between the CaBP1 C lobe and residues within the SD contribute further to high-affinity binding of CaBP1 (18). The hydrophobic interactions between CaBP1 and the IBC are essential for CaBP1 binding and inhibition of InsP₃R (Fig. 3 and Figs. S1F and S5). Docking the NT–CaBP1 complex into the structure of a full-length InsP₃R reveals an arrangement in which tetrameric CaBP1 is anchored by its hydrophobic contacts to the underlying NT domains. CaBP1 thereby forms a ring-like structure around the cytosolic vestibule that leads to the InsP₃R pore (Fig. 2B). This arrangement has the Ca²⁺-binding sites of CaBP1 lining the route through which Ca²⁺ passes via the InsP₃R to the cytosol (Fig. 2B and C).

The InsP₃-induced conformational change that initiates InsP₃R activation involves rearrangement of an interface between the SD and IBC-β domain. This intrasubunit rearrangement then disrupts an interaction between subunits mediated by the HS loop of the SD (29). This loop includes a residue (Y167 in InsP₃R1) that is important for gating of InsP₃Rs (38) and ryanodine receptors (39). Our cross-linking analyses support this scheme because residues that contribute to the intersubunit interface are less readily cross-linked in the presence of InsP₃ (Fig. 4B and Fig. S6E). Ca²⁺–CaBP1 has the opposite effect: It increases cross-linking (Fig. 4) and inhibits InsP₃R gating by stabilizing a closed

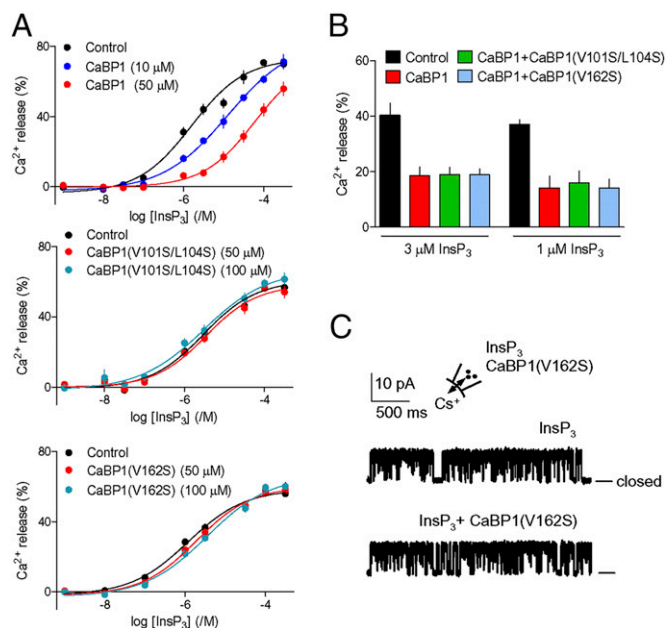
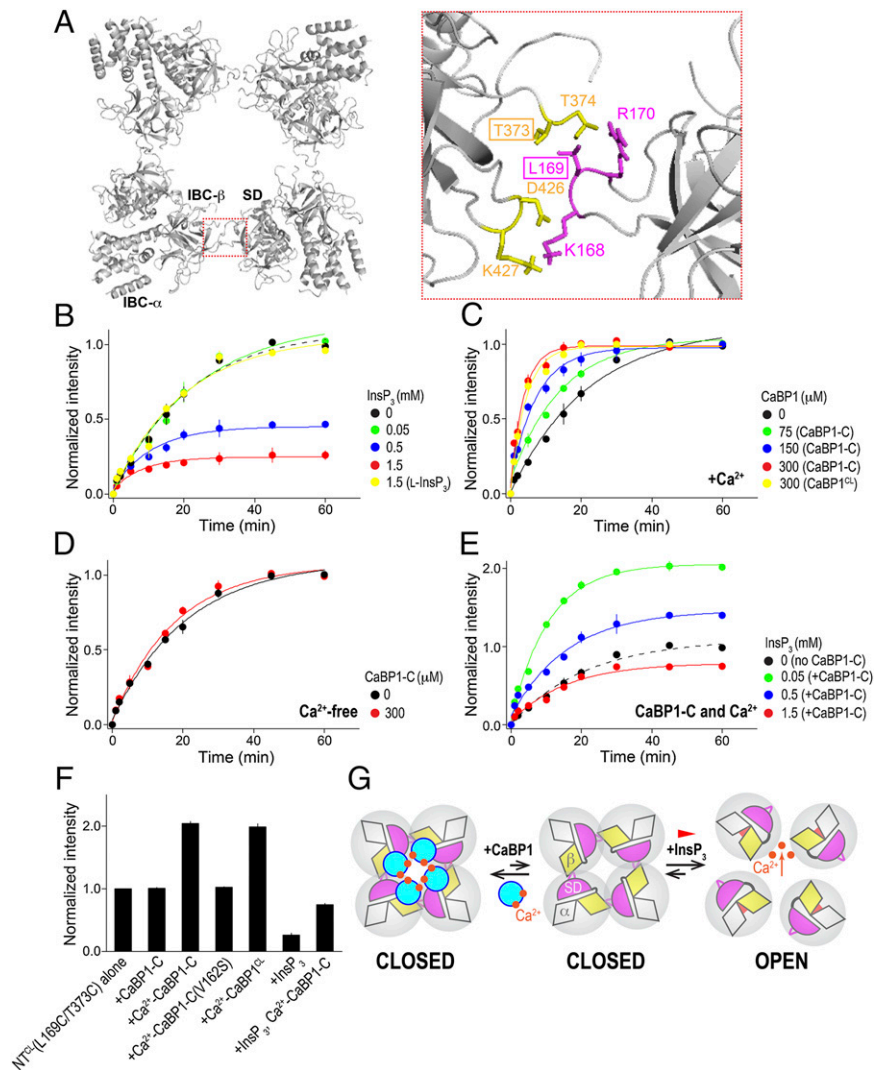


Fig. 3. Hydrophobic residues in CaBP1 are essential for inhibition of InsP₃R. (A) Inhibition of InsP₃-evoked Ca²⁺ release by CaBP1 is abolished after mutation of its key hydrophobic residues. Permeabilized DT40–InsP₃R1 cells in CLM with [Ca²⁺]_c of 3.5 μM were incubated with the indicated concentrations of CaBP1, CaBP1(V162S), or CaBP1(V101S/L104S) (10 min) before adding InsP₃. Results show the concentration-dependent release of Ca²⁺ by InsP₃. (B) Ca²⁺ release evoked by 1 or 3 μM InsP₃ alone, with CaBP1 (50 μM), or with CaBP1 (50 μM) and mutant CaBP1 (100 μM). Results (A and B) are means ± SEM; n = 4, with duplicate determinations in each. Similar results performed in CLM with 1.2 μM [Ca²⁺]_c are shown in Fig. S5D and E. Summary results are in Table S3. (C) Typical patch-clamp recordings from single InsP₃R1 in medium with [Ca²⁺]_c of 1.5 μM stimulated with InsP₃ (10 μM) alone or in combination with CaBP1(V162S) (10 μM) shows that the mutant CaBP1 is inactive. Bars show the closed state. The holding potential was +40 mV. Summary results are shown in Fig. S1F. Fig. 2A shows the positions of mutated residues.

Fig. 4. Opposing effects of CaBP1 and InsP₃ on interactions between NTs. (A) Top view of the tetrameric structure of NTs, and close-up view of the boxed area of the intersubunit interface between the HS loop of the SD (magenta) and IBC-β (yellow) (29). The two residues that were replaced by Cys for CuP cross-linking analyses are boxed. (B) InsP₃ weakens the interactions between NT subunits and thereby the rate of CuP-mediated cross-linking of tetrameric NT. NT^{CL}(L169C/T373C) (75 μM) in medium containing 5 mM CaCl₂ was incubated with CuP (100 μM) alone or with the indicated concentrations of InsP₃ (the naturally occurring D-isomer) or biologically inactive L-InsP₃. Results are expressed as fractions of the average intensity of the tetramer band detected at 60 min in the control incubation (no InsP₃). The results with NT^{CL}(L169C/T373C) alone (black) are shown for comparison. (C and D) Similar cross-linking experiments show that CaBP1 has the opposite effect to InsP₃. Effects on tetramer formation of the indicated concentrations of the C lobe of CaBP1 (CaBP1-C) and of the Cys-less form of full-length CaBP1 (CaBP1^{CL}) in medium containing 5 mM CaCl₂ (C) or in Ca²⁺-free medium (D). (E) The C-terminal of CaBP1 substantially blocks the destabilization of NT subunit interactions by InsP₃. Effects of the indicated concentrations of InsP₃ with CaBP1 C lobe (300 μM) in medium containing 5 mM CaCl₂. Results are expressed as fractions of the average intensity of the tetramer band detected at 60 min in the control incubation (no InsP₃ or CaBP1). The results with NT^{CL}(L169C/T373C) alone (black) are shown for comparison. (F) Summary data show amounts of cross-linked NT^{CL}(L169C/T373C) tetramer detected at 60 min relative to NT^{CL}(L169C/T373C) alone at 60 min. Results in B–F show means ± standard deviation from three independent experiments. InsP₃ denotes D-InsP₃ unless indicated otherwise. The data from which these analyses derive are shown in Fig. S6, and the rate constants and normalized band intensities in Table S4. (G) Interactions between adjacent NTs mediated by IBC-β (yellow) and the HS loop of the SD (magenta) hold the tetrameric InsP₃R in a closed state. InsP₃ binding closes the clam-like IBC, disrupting these intersubunit interactions, and allowing the channel to open. The cytosolic vestibule of the InsP₃R with four CaBP1s (cyan) bound is probably at least 5 Å across and unlikely to impede the flow of ions. Instead, we suggest that CaBP1 clamps the intersubunit interactions and thereby inhibits channel opening.



state of the channel (Fig. 1). We suggest that CaBP1 counteracts the InsP₃-induced conformational change by “clamping” the underlying InsP₃R subunits and restricting their relative motion. We speculate that CaBP1 held loosely to neuronal InsP₃R at resting [Ca²⁺]_c tightens its grip as Ca²⁺ passing through an open InsP₃R binds to CaBP1 to cause rapid feedback inhibition (Fig. 4G).

Materials and Methods

Expression and Purification of CaBP1, NT, and Their Mutants. The short form of CaBP1 was used throughout. CaBP1 and its mutants were expressed and purified from *Escherichia coli* strain BL21(DE3) as described (40). NT (residues 1–604) and NT^{CL} (in which native Cys are replaced by Ala) from rat InsP₃R1 were expressed and purified as described (29, 41). Individual Cys residues were introduced into NT^{CL} using the QuikChange site-directed mutagenesis kit. Sequences of all plasmids were confirmed. Table S1 lists the proteins used.

NMR Spectroscopy. Samples were prepared by dissolving perdeuterated and uniformly ¹⁵N/¹³C-labeled CaBP1 (0.2 mM) containing protonated methyl groups (for Val, Leu, and Ile) (42) in 0.3 mL of 95% [²H]₂O containing 10 mM [²H₁₁]Tris, pH 7.4, 0.1 mM KCl, and either 5 mM EDTA or 5 mM CaCl₂ in the presence of 0.2 mM NT^{CL} or NT^{CL} with single Cys substitutions (E20C, A61C, R170C, H289C, N300C, A394C, and K424C). Methyl TROSY experiments on ¹³C-labeled CaBP1 bound to unlabeled NT^{CL} were performed as described

(43). NMR-PRE experiments were performed on samples that contained isotopically labeled CaBP1 bound to NT^{CL} with a single Cys insertion with or without an attached nitroxide spin label. Spin labeling was performed as described (31). All NMR experiments were performed at 30 °C on a Bruker Avance 800 MHz spectrometer equipped with triple-resonance cryoprobe and z axis gradient. NMR assignments were described (18).

Molecular Docking. Atomic coordinates for the NT (PDB ID code 3UG4) and CaBP1 C lobe (PDB ID code 2K7D) were used to generate the docked structure in Fig. 2A. For docking of full-length CaBP1 to NT (Fig. 2C), an ensemble of structures of full-length CaBP1 (with a flexible linker between the two lobes) was generated by a simulated annealing protocol within CYANA using distance restraints derived for the CaBP1 C lobe and N lobe (PDB ID code 2K7B). All docking calculations were performed by using the HADDOCK Guru interface (<http://haddock.science.uu.nl/services/HADDOCK/haddock.php>) (44). Mutagenesis data and chemical-shift perturbation data were used as inputs to define active and passive residues to generate ambiguous restraints (44). The PRE ratios (Fig. S4C) were converted into unambiguous restraints and docking calculations were performed as described (45). The final docked structure in Fig. 2A is the average of 148 calculated structures that converged within a single cluster (red dots in Fig. S4D).

InsP₃-Evoked Ca²⁺ Release and ³H-InsP₃ Binding. DT40 cells stably expressing only rat InsP₃R1 (DT40-InsP₃R1 cells) were loaded with a low-affinity luminal Ca²⁺ indicator, permeabilized in cytosol-like medium (CLM), and the Ca²⁺ content of the endoplasmic reticulum was continuously monitored during

additions of ATP (to allow Ca^{2+} uptake), CaBP1, and InsP_3 as described (46). Ca^{2+} release evoked by InsP_3 is expressed as a percentage of the ATP-dependent Ca^{2+} uptake. $^3\text{H-InsP}_3$ binding to rat cerebellar membranes or purified NT was performed in CLM at 4 °C as described (28). Results were fitted to Hill equations.

Patch-Clamp Recording. Currents were recorded from patches excised from the outer nuclear envelope of DT40- $\text{InsP}_3\text{R1}$ cells by using symmetrical cesium methanesulfonate (140 mM) as charge carrier. The composition of recording solutions and methods of analysis were otherwise as described (47).

Cross-Linking of Cys Residues. For CuP cross-linking, a mixture of 50 mM CuSO_4 and 65 mM 1,10-phenanthroline (Sigma) was freshly prepared. Concentrations in the text refer to final CuP concentration ($\geq 50 \mu\text{M}$). NT^{CL} or its mutants (75 μM) were incubated on ice with CuP in medium containing 360 mM NaCl, 20 mM Tris-HCl, pH 8.4, 2.5% (vol/vol) glycerol, and 0.2 mM Tris(2-carboxyethyl)phosphine (TCEP). Ca^{2+} -free buffer was prepared by using Chelex 100 resin (Bio-Rad Laboratories). NT^{CL} (L169C/T373C) and CaBP1 C lobe were used after dialysis in Ca^{2+} -free buffer. Reactions were

quenched by addition of 10 mM *N*-ethylmaleimide and 10 mM EDTA (final concentrations). Samples were mixed with 4× nonreducing SDS loading buffer, heated at 55 °C for 15 min, and subjected to SDS/PAGE by using NuPAGE 3–8% Tris-acetate gels (Invitrogen). After Coomassie Brilliant Blue staining, band intensities of tetrameric NT were quantified by densitometry using ImageJ. For analyses of time courses, the intensity of the tetramer band at each time for the experimental condition was expressed relative to the intensity of the tetramer band at 60 min for control condition (no InsP_3 or CaBP1). These normalized intensities were fitted with a single exponential time course by using IGOR Pro-6 (WaveMetrics).

ACKNOWLEDGMENTS. We thank Dr. Jerry Dallas for help with NMR experiments. This work was supported by National Institutes of Health Grants EY012347 and NS045909 (to J.B.A.) and RR11973 (to the University of California at Davis NMR Facility); Canadian Institutes of Health Research (CIHR) and the Canada Foundation for Innovation grants (to M.I.); Wellcome Trust Grant 085295; Biotechnology and Biological Sciences Research Council Grant BB/H009736/1 (to C.W.T.). A.M.R. is a Fellow of Queens' College. T.R. was a Fellow of Pembroke College.

- Berridge MJ, Bootman MD, Roderick HL (2003) Calcium signalling: Dynamics, homeostasis and remodelling. *Nat Rev Mol Cell Biol* 4(7):517–529.
- Haynes LP, McCue HV, Burgoyne RD (2012) Evolution and functional diversity of the Calcium Binding Proteins (CaBPs). *Front Mol Neurosci* 5:e9.
- Barbara JG (2002) IP_3 -dependent calcium-induced calcium release mediates bidirectional calcium waves in neurons: Functional implications for synaptic plasticity. *Biochim Biophys Acta* 1600(1–2):12–18.
- Taylor CW, Dale P (2012) Intracellular Ca^{2+} channels—a growing community. *Mol Cell Endocrinol* 353(1–2):21–28.
- Foskett JK, White C, Cheung KH, Mak DO (2007) Inositol trisphosphate receptor Ca^{2+} release channels. *Physiol Rev* 87(2):593–658.
- Taylor CW, Tovey SC (2010) IP_3 receptors: Toward understanding their activation. *Cold Spring Harb Perspect Biol* 2(12):a004010.
- Konieczny V, Keebler MV, Taylor CW (2012) Spatial organization of intracellular Ca^{2+} signals. *Semin Cell Dev Biol* 23(2):172–180.
- Miyakawa T, et al. (2001) Ca^{2+} -sensor region of IP_3 receptor controls intracellular Ca^{2+} signaling. *EMBO J* 20(7):1674–1680.
- Taylor CW, Laude AJ (2002) IP_3 receptors and their regulation by calmodulin and cytosolic Ca^{2+} . *Cell Calcium* 32(5–6):321–334.
- Adkins CE, et al. (2000) Ca^{2+} -calmodulin inhibits Ca^{2+} release mediated by type-1, -2 and -3 inositol trisphosphate receptors. *Biochem J* 345(Pt 2):357–363.
- Michikawa T, et al. (1999) Calmodulin mediates calcium-dependent inactivation of the cerebellar type 1 inositol 1,4,5-trisphosphate receptor. *Neuron* 23(4):799–808.
- Patel S, Morris SA, Adkins CE, O'Beirne G, Taylor CW (1997) Ca^{2+} -independent inhibition of inositol trisphosphate receptors by calmodulin: Redistribution of calmodulin as a possible means of regulating Ca^{2+} mobilization. *Proc Natl Acad Sci USA* 94(21):11627–11632.
- White C, Yang J, Monteiro MJ, Foskett JK (2006) CIB1, a ubiquitously expressed Ca^{2+} -binding protein ligand of the InsP_3 receptor Ca^{2+} release channel. *J Biol Chem* 281(30):20825–20833.
- Schlecker C, et al. (2006) Neuronal calcium sensor-1 enhancement of InsP_3 receptor activity is inhibited by therapeutic levels of lithium. *J Clin Invest* 116(6):1668–1674.
- Yang J, et al. (2002) Identification of a family of calcium sensors as protein ligands of inositol trisphosphate receptor Ca^{2+} release channels. *Proc Natl Acad Sci USA* 99(11):7711–7716.
- Kasri NN, et al. (2004) Regulation of InsP_3 receptor activity by neuronal Ca^{2+} -binding proteins. *EMBO J* 23(2):312–321.
- Haeseleer F, et al. (2000) Five members of a novel Ca^{2+} -binding protein (CABP) subfamily with similarity to calmodulin. *J Biol Chem* 275(2):1247–1260.
- Li C, et al. (2009) Structural insights into Ca^{2+} -dependent regulation of inositol 1,4,5-trisphosphate receptors by CaBP1. *J Biol Chem* 284(4):2472–2481.
- Findeisen F, Minor DL, Jr. (2010) Structural basis for the differential effects of CaBP1 and calmodulin on $\text{Ca}_v1.2$ calcium-dependent inactivation. *Structure* 18(12):1617–1631.
- Haynes LP, Tepikin AV, Burgoyne RD (2004) Calcium-binding protein 1 is an inhibitor of agonist-evoked, inositol 1,4,5-trisphosphate-mediated calcium signaling. *J Biol Chem* 279(1):547–555.
- Menger N, Seidenbecher CI, Gundelfinger ED, Kreutz MR (1999) The cytoskeleton-associated neuronal calcium-binding protein caldendrin is expressed in a subset of amacrine, bipolar and ganglion cells of the rat retina. *Cell Tissue Res* 298(1):21–32.
- Seidenbecher CI, Reissner C, Kreutz MR (2002) Caldendrins in the inner retina. *Adv Exp Med Biol* 514:451–463.
- Lee A, et al. (2002) Differential modulation of $\text{Ca}_v2.1$ channels by calmodulin and Ca^{2+} -binding protein 1. *Nat Neurosci* 5(3):210–217.
- Zhou H, Yu K, McCoy KL, Lee A (2005) Molecular mechanism for divergent regulation of $\text{Ca}_v1.2$ Ca^{2+} channels by calmodulin and Ca^{2+} -binding protein-1. *J Biol Chem* 280(33):29612–29619.
- Kinoshita-Kawada M, et al. (2005) Inhibition of TRPC5 channels by Ca^{2+} -binding protein 1 in *Xenopus* oocytes. *Pflügers Arch* 450(5):345–354.
- Bosanac I, et al. (2002) Structure of the inositol 1,4,5-trisphosphate receptor binding core in complex with its ligand. *Nature* 420(6916):696–700.
- Bosanac I, et al. (2005) Crystal structure of the ligand binding suppressor domain of type 1 inositol 1,4,5-trisphosphate receptor. *Mol Cell* 17(2):193–203.
- Rossi AM, et al. (2009) Synthetic partial agonists reveal key steps in IP_3 receptor activation. *Nat Chem Biol* 5(9):631–639.
- Seo MD, et al. (2012) Structural and functional conservation of key domains in InsP_3 and ryanodine receptors. *Nature* 483(7387):108–112.
- Rahman T, Taylor CW (2010) Nuclear patch-clamp recording from inositol 1,4,5-trisphosphate receptors. *Methods Cell Biol* 99:199–224.
- Clore GM, Tang C, Iwahara J (2007) Elucidating transient macromolecular interactions using paramagnetic relaxation enhancement. *Curr Opin Struct Biol* 17(5):603–616.
- Dominguez C, Boelens R, Bonvin AM (2003) HADDOCK: A protein-protein docking approach based on biochemical or biophysical information. *J Am Chem Soc* 125(7):1731–1737.
- Ikura M (1996) Calcium binding and conformational response in EF-hand proteins. *Trends Biochem Sci* 21(1):14–17.
- Ludtke SJ, et al. (2011) Flexible architecture of $\text{IP}_3\text{R1}$ by cryo-EM. *Structure* 19(8):1192–1199.
- Tung CC, Lobo PA, Kimlicka L, Van Petegem F (2010) The amino-terminal disease hotspot of ryanodine receptors forms a cytoplasmic vestibule. *Nature* 468(7323):585–588.
- Zhang M, Tanaka T, Ikura M (1995) Calcium-induced conformational transition revealed by the solution structure of apo calmodulin. *Nat Struct Biol* 2(9):758–767.
- Gagné SM, Tsuda S, Li MX, Smillie LB, Sykes BD (1995) Structures of the troponin C regulatory domains in the apo and calcium-saturated states. *Nat Struct Biol* 2(9):784–789.
- Yamazaki H, Chan J, Ikura M, Michikawa T, Mikoshiba K (2010) Tyr-167/Trp-168 in type 1/3 inositol 1,4,5-trisphosphate receptor mediates functional coupling between ligand binding and channel opening. *J Biol Chem* 285(46):36081–36091.
- Amador FJ, et al. (2009) Crystal structure of type I ryanodine receptor amino-terminal beta-trefoil domain reveals a disease-associated mutation “hot spot” loop. *Proc Natl Acad Sci USA* 106(27):11040–11044.
- Wingard JN, et al. (2005) Structural analysis of Mg^{2+} and Ca^{2+} binding to CaBP1, a neuron-specific regulator of calcium channels. *J Biol Chem* 280(45):37461–37470.
- Chan J, et al. (2007) Ligand-induced conformational changes via flexible linkers in the amino-terminal region of the inositol 1,4,5-trisphosphate receptor. *J Mol Biol* 373(5):1269–1280.
- Tugarinov V, Kay LE (2004) An isotope labeling strategy for methyl TROSY spectroscopy. *J Biomol NMR* 28(2):165–172.
- Tugarinov V, Sprangers R, Kay LE (2004) Line narrowing in methyl-TROSY using zero-quantum ^1H - ^{13}C NMR spectroscopy. *J Am Chem Soc* 126(15):4921–4925.
- de Vries SJ, van Dijk M, Bonvin AM (2010) The HADDOCK web server for data-driven biomolecular docking. *Nat Protoc* 5(5):883–897.
- Battiste JL, Wagner G (2000) Utilization of site-directed spin labeling and high-resolution heteronuclear nuclear magnetic resonance for global fold determination of large proteins with limited nuclear overhauser effect data. *Biochemistry* 39(18):5355–5365.
- Tovey SC, Sun Y, Taylor CW (2006) Rapid functional assays of intracellular Ca^{2+} channels. *Nat Protoc* 1(1):259–263.
- Taufiq-Ur-Rahman, Skupin A, Falcke M, Taylor CW (2009) Clustering of InsP_3 receptors by InsP_3 retunes their regulation by InsP_3 and Ca^{2+} . *Nature* 458(7238):655–659.